

Rheofluorescence Technique for the Study of Dilute MEH-PPV Solutions in Couette Flow

Elisabeth K. Hill,^{1,2} Richard L. Watson,¹ and Dave E. Dunstan¹

Received October 29, 2004; revised February 3, 2005; accepted February 7, 2005

A novel rheofluorescence technique has been developed that permits the study of fluorescent polymers in a near-uniform shear field. The system has been used to examine the effects of shear flow on dilute solutions of two commercially available samples of poly[2-methoxy-5-(2-ethylhexyloxy)-1,4-phenylenevinylene] (MEH-PPV) in toluene and xylene. A detailed description of the instrument is provided, along with data that confirm a small probe molecule, Rhodamine 6G, is not affected by simple shear flow. MEH-PPV solutions were examined over two decades of concentration for rheochromism indicative of changes in segment length, and shear-induced orientation revealed by measurements of the steady state emission anisotropy. It is demonstrated that these dilute samples were not influenced by shear rates in the range 100–1000 s⁻¹. In contrast, MEH-PPV dispersed in a concentrated polystyrene solution showed evidence of shear-induced orientation and rheochromism. This new technique shows promise for investigating the impact of shear flow on the conformation of conjugated polymers employed in organic optoelectronic devices.

KEY WORDS: MEH-PPV; shear flow; couette cell; rheofluorescence.

INTRODUCTION

The fortuitous discovery of electroluminescence from conjugated polymers [1] precipitated explosive interest in the development of polymer light emitting diodes and other optoelectronic devices. [2] Today many groups worldwide are working to understand and optimize device performance, spurred on by numerous applications in display technology. [3] Microstructural control of polymer chain conformation and packing in luminescent active layers has emerged as a critical requirement for high performance displays. [4,5] Debate continues regarding the exact nature of the photophysical processes involved, but it is already clear that polymer-processing conditions play a large part in determining device characteristics. Two popular methods for film deposition, namely spin coating and ink-jet printing, expose the polymer to high

shear rate regimes, [6] however little is known about the effects of shear on chain conformation and association in these complex systems.

Polymer conformation and orientation in flow has been widely studied using rheological and rheo-optic techniques, and the reader is referred to the literature for reviews of this field. [7–9] Our own work has included studies of conducting polymers and polyelectrolytes in simple shear flow using UV-visible absorption spectroscopy. [10–12] In the quiescent state, fluorescence techniques have proven a valuable tool to elucidate the conformation and dynamics of polymer systems, by means of judiciously chosen fluorescent tags or labels. [13–15] Fluorescence measurements of polymers in shear flow therefore seem a natural, and pertinent, extension to existing rheo-optic techniques, [16] and particularly well-suited to studies of luminescent conjugated polymers. Yet reports of such rheofluorescence experiments—i.e., the determination of fluorescence emission characteristics in shear flow—have been confined to a handful of groups and systems.

Bur and co-workers described an optically transparent cone and plate geometry employed for fluorescence

¹ Department of Chemical and Biomolecular Engineering, The University of Melbourne, VIC, 3010, Australia.

² To whom correspondence should be addressed. E-mail: e.hill@unimelb.edu.au

anisotropy measurements of anthracene-labeled polybutadiene doped in a polybutadiene melt. [17] Mani *et al.* investigated the effects of shear flow on the phase behavior of a two-species polymer blend using fluorescence quenching of anthracene-labeled polystyrene as an indicator of miscibility. [18] More recently, single-molecule visualization techniques have permitted the observation of large, fluorescently labeled, DNA molecules in steady shear [19] and extensional flow, [20] and a synthetic polymer, dansyl-labeled polyacrylamide, in a parallel plate geometry. [21]

Rotating parallel plate configurations generate a shear field that varies with radial displacement from the axis of rotation; therefore spatially resolved fluorescence measurements are required in order to correlate observed deformations with applied shear. In contrast, a Couette cell, comprising two concentric cylinders, can generate a uniform shear field. This is achieved in the narrow gap limit, when rotation of one cylinder relative to the other generates a linear velocity gradient, and constant shear rate, across the gap. [22] Material introduced to the gap between the cylinders consequently experiences a near-uniform shear rate independent of position. A judicious choice of optical elements also permits interrogation along several axes relative to the flow direction. We therefore selected the Couette format for our rheofluorescence measurements because of the spatially uniform shear field and the ability to examine distinct observation axes defined by the flow geometry.

Fluorescence spectroscopy [23] has the potential to report on a diverse range of polymer characteristics in shear, depending on the selection of chromophore and environment. The sensitivity of this technique means that low concentrations of fluorescent polymer may be used in dilute solution or as a non-perturbing probe in more concentrated systems. Simple changes in emission intensity may reveal a change in absorption cross-section resulting from shear-induced orientation, providing the fluorescence quantum efficiency is unaltered. Rheochromism, a shear-induced shift in emission wavelength, can be caused by a shear-induced change in the distribution of segment lengths in a conjugated polymer. Polarized fluorescence studies offer further insight into orientational aspects of polymer behavior; these measurements exploit the fact that absorption and emission transition moments have a defined orientation with respect to the molecular axis, and can therefore reveal shear-induced alignment. Second order measurements, for example, fluorescent resonance energy transfer (FRET) between donor-acceptor pairs, quenching, and fluorescence recovery after photobleaching (FRAP), also have their place in the armory.

Poly[*p*-phenylenevinylene] derivatives are an important class of solution processable conjugated polymers that show promise for polymer optoelectronic displays. Of these, poly[2-methoxy-5-(2-ethylhexyloxy)-1,4-phenylenevinylene] (MEH-PPV) has emerged as a useful archetype, and has been extensively studied. [4,24] It is a highly fluorescent polymer comprising conjugated *p*-phenylenevinylene units with sidechains that render it soluble in common aprotic solvents. The chromophores consist of conjugated segments of the polymer backbone acting as a single optical unit, thereby offering a direct correlation between observed emission and polymer conformation and environment. The conformation of the conjugated polymer chain has been shown to affect morphology and interchain interactions in thin films; [4] of particular note is the study by Nguyen *et al.* that revealed the importance of MEH-PPV solution conformation in “memory effects” in films. [25]

Accordingly, this work develops a method to study the effects of simple shear flow on luminescent conjugated polymers, employing MEH-PPV as an exemplar. Fluorescence techniques are ideally suited to this problem. A novel, optically accessible Couette cell has been developed and characterized with a small molecule probe known to be unaffected by simple shear flow. The present study is primarily restricted to dilute solutions, *i.e.*, those in which the polymer chains do not interact, and aggregation is minimal. This constraint enables us to focus exclusively on the shear-induced response of discrete macromolecular chains.

EXPERIMENTAL DETAILS

Materials and Methods

Poly[2-methoxy-5-(2-ethylhexyloxy)-1,4-phenylenevinylene] (MEH-PPV) was obtained from two commercial sources: American Dye Source Inc., Quebec, Canada, (weight average molecular weight, $M_w \sim 9.8 \times 10^5 \text{ g}\cdot\text{mol}^{-1}$, polydispersity index ~ 8.8 , hereafter referred to as 980 k MEH-PPV) and Sigma-Aldrich Pty. Ltd., Castle Hill, Australia ($M_w \sim 1.33 \times 10^5 \text{ g}\cdot\text{mol}^{-1}$, polydispersity index ~ 1.06 , denoted as 133 k MEH-PPV). Both polymers were stored in the dark at 4°C and used as received. MEH-PPV stock solutions were prepared in toluene or xylene at typically 0.1–0.2 mg·ml⁻¹. Dissolution was completed by warming to 60°C for several hours, until no more polymer flecks were visible and the reddish-orange solution appeared homogenous. Solutions were sealed and stored in the dark until required. Working solutions were prepared by volumetric dilution from the stock

and used promptly. Solution stability was checked using UV-vis absorption spectroscopy. Absorption and emission spectra for solutions of both polymers were comparable in form and intensity. Any alteration in the molar absorption coefficient or the form of the spectrum indicated deterioration of the sample, which was not used for further study.

A dispersion of MEH-PPV in concentrated polystyrene solution was prepared by dissolving polystyrene granules ($M_w \sim 3.5 \times 10^5 \text{ g}\cdot\text{mol}^{-1}$, polydispersity index ~ 2.1 , Sigma-Aldrich) in a solution of 133 k MEH-PPV in toluene to yield a final composition of 1×10^{-3} wt.-% MEH-PPV and 16.2 wt.-% polystyrene in toluene. This solution was agitated gently on a roller mixer for 48 hr to achieve homogeneity.

Rhodamine 6G was from Sigma-Aldrich (Fluka Standard) and used as received. All solvents were analytical or spectroscopic grade, checked for absorption or fluorescence in the region of interest, and used without further purification. Xylene was a mixture of the 1,2- 1,3- and 1,4-isomers. Solvent refractive indices were determined using a Bellingham and Stanley refractometer.

Fluorescence measurements were performed with a steady state fluorescence spectrophotometer (Cary Eclipse; Varian Inc., Melbourne, Australia) calibrated in accordance with the manufacturer's guidelines. It was equipped with a manual thin film polarizer accessory for depolarization studies. A Cary 3E UV-vis spectrophotometer (Varian Inc.) was used for absorption analyses. Bulk solutions were examined in 2 mm or 10 mm path length quartz cuvettes (Starna Pty. Ltd., Thornleigh, Australia). Fluorescence emission anisotropy, as defined in Equation (1) for the isotropic case in a right-angled geometry, was determined from polarized fluorescence measurements in order to investigate reductions in rotational freedom.

$$r = \frac{I_{VV} - GI_{VH}}{I_{VV} + 2GI_{VH}}; \quad G = \frac{I_{HV}}{I_{HH}} \quad (1)$$

Rheofluorescence Cell

Shear cell experiments were undertaken in an optically accessible Couette cell comprising two concentric cylinders. A schematic diagram of the specially-developed rheo-optical apparatus is given in Fig. 1. The Couette geometry is generated in a polished quartz block with a 10.00 mm hole bored vertically through the center. A Teflon[®] inner cylinder (diameter 9.65 mm) passes through the center of the hole. This through-cell arrangement minimizes end effects present in the conventional cup-and-bob design, and reduces the risk of trapping air bubbles in the system. Sample solutions are carefully in-

troduced to the gap between the cylinders, and tight-fitting seals prevent leakage. Less than 0.25 cm³ polymer solution is required to completely fill the cell. Concentricity is ensured in a self-centering device that locks the cell in place, and controlled rotation of the inner cylinder generates a well-behaved shear field.

An external toothed belt mechanism is employed to drive the rotating cylinder. Use of this belt isolates the shear cell from small off-axis perturbations of the motor shaft and improves alignment consistency. The rotational speed of the drive motor (RS Components, Northampton, UK) is continuously adjustable, and a reciprocal counter (Thurlby Thandar Instruments PFM 1300, Cambridgeshire, UK) is connected to the motor to report instantaneous rotational frequency. A series of calibrations were completed to relate the rate displayed by the counter to the true rotational frequency of the inner cylinder inside the Couette cell.

In the narrow gap limit, the shear rate experienced by the sample between the cylinders may be determined according to the standard simplified expression given in Equation (2):

$$\dot{\gamma} = \frac{2\Omega}{1 - (R_1/R_2)^2} \quad (2)$$

where $\dot{\gamma}$ is the shear rate, Ω the angular velocity of the inner cylinder in $\text{rad}\cdot\text{s}^{-1}$, and R_1 , R_2 are the radii of the inner and outer cylinders respectively. [22] In our configuration, the radius ratio of the two cylinders (0.965) generates less than 8% variation in $\dot{\gamma}$ across the gap, [26,27] and the maximum accessible shear rate is approximately 1200 s^{-1} . Earlier work undertaken with $0.3 \mu\text{m}$ tracer particles on a comparable system in this laboratory indicated that laminar flow is maintained well above the shear rate ranges employed in this study, in accord with theoretical predictions. [27,28]

The entire optical assembly is designed to fit in the sample compartment of the fluorescence spectrometer. XY translation stages permit precise alignment of the cell with respect to the excitation and detection axes, as illustrated in Fig. 1. (inset). The classical right-angled excitation/detection geometry is retained in order to minimize stray scattered light and simplify depolarization experiments. (Alternative optical configurations, e.g., front face illumination, require the inclusion of a dichroic beam splitter to discriminate between excitation and emission wavelengths. These interference filters introduce an additional polarization-dependent response that compromises anisotropy measurements, and are best avoided.) The excitation region is approximately halfway along the cell's vertical axis, to avoid any distortions in the shear field due to end effects. Two principal

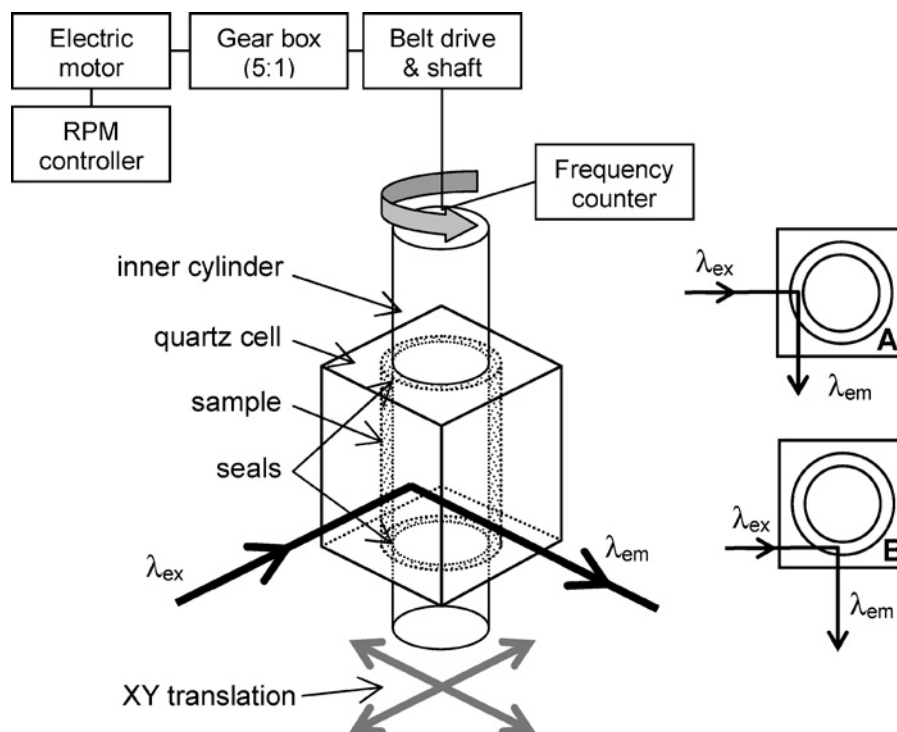


Fig. 1. Schematic diagram showing the Couette cell and apparatus used for fluorescence measurements in shear. The inset illustrates the relative location of the two observation positions in the cell: excitation across flow (A), and excitation along the flow direction (B).

observation positions are accessible when the solvent refractive index matches, or is greater than, the refractive index of fused silica ($n = 1.46$). In Position A, an excitation beam passes across the flow direction, whilst in Position B illumination is tangential to the flow. Total internal reflection renders Position B optically inaccessible when $n_{\text{solvent}} < n_{\text{silica}}$.

The excitation beam is focused by the spectrometer to a 1 mm round spot in the flow cell. Two principal modes of fluorescence measurement are available; conventional excitation and emission scans, and continuous monitoring of emission intensity observed from a given combination of excitation and emission wavelengths.

RESULTS AND DISCUSSION

Characterization with Rhodamine 6G

The rheofluorescence instrument was first assessed using a series of dilute solutions of Rhodamine 6G in water, ethanol and glycerol/water mixtures of varying composition and viscosity. This small dye molecule has very well-characterized photophysics, [29–32] and was not anticipated to show any orientation effects in steady shear

flow. It provided an effective probe to confirm instrumental performance, and establish sensitivity limits.

Solutions were all prepared by serial dilution from an ethanolic stock into the solvent system of choice. Homogeneity in the more viscous systems was assured by ultrasonication or roller mixing. All working solutions had an optical density of less than 0.1 cm^{-1} in a quartz cuvette and quiescent absorption and emission spectra were in accord with established data. Studies of the effect of shear rate on emission intensity showed no dependence although they highlighted the impact of instrumental drift during measurement series lasting in excess of one hour. (Intensity changes of up to $5\% \cdot \text{h}^{-1}$ “were observed.”).

Measurements with polarized light demonstrated no change in steady state emission anisotropy with shear, as illustrated in Fig. 2, for $0.5 \mu\text{M}$ Rhodamine 6G in 80 wt.% glycerol/water. This behavior is as expected for a small dye molecule, for which rotational diffusion is the predominant depolarization mechanism. The invariance of the measured anisotropy value with shear rate also indirectly confirms the absence of thermal effects in the Couette cell. Heat transfer to the solution resulting from rotation of the inner cylinder is negligible. If this were not the case, the anisotropy values would show a variation

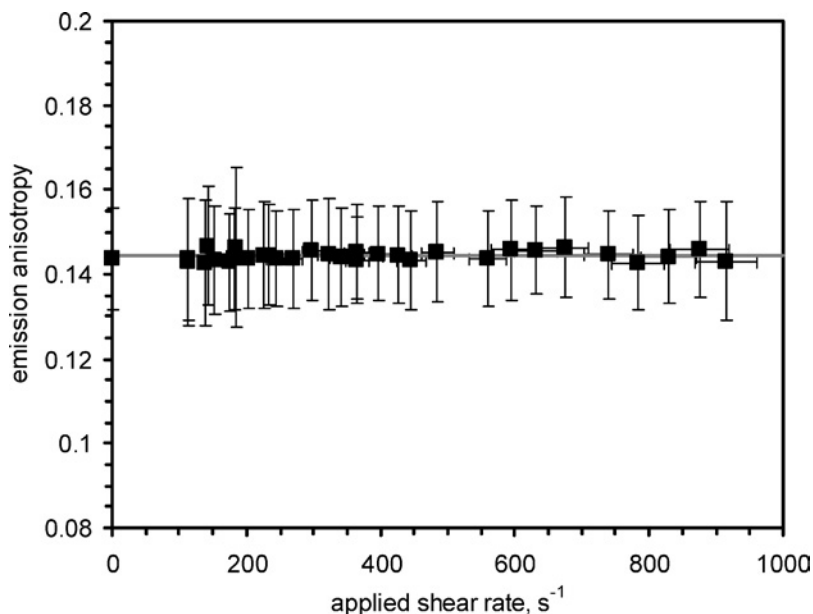


Fig. 2. Invariance of steady state fluorescence anisotropy with shear. $0.5 \mu\text{M}$ Rhodamine 6G in 80 wt.-% glycerol/water. $\lambda_{\text{ex}} = 530 \text{ nm}$, $\lambda_{\text{em}} = 555 \text{ nm}$. The gray line indicates the mean anisotropy value; excitation was across the flow axis (Position A). Error bar magnitudes were determined by compounding percentage errors (one standard deviation) for each individual polarized intensity measurement.

with shear rate that correlates with the temperature dependence of rotational diffusion described by the Perrin equation. [23]

The error margins for anisotropy presented in Fig. 2 are larger than those typically reported for static measurements. (± 0.005 or better.) This is because rotation of the inner cylinder introduces additional uncertainty in the intensity values for each polarization combination, which is compounded in the anisotropy calculation (Equation (1)). It was further observed that values for r and G determined in the rheofluorescence cell were not identical to values determined in a conventional quartz cuvette. The reasons for this discrepancy are described in more detail below, but were traced to a combination of lensing effects in the cylindrical cell, and scatter from the surface of the Teflon[®] inner cylinder. Wavelength resolution in the emission spectra was also slightly reduced for the same reasons.

We therefore conclude that the rheofluorescence instrument is sufficiently sensitive to detect fluorescent emission from dilute (sub-micromolar) solutions of interest. Measurements are not distorted by shear-induced heating of the sample solution, but are limited by the intrinsic thermal stability of the spectrometer, and optical characteristics of the Couette cell. These constraints are not critical; they should merely inform ex-

perimental design and data interpretation in the polymer investigations.

Dilute MEH-PPV Solutions in Shear Flow

MEH-PPV is a highly fluorescent, conjugated polymer with side chains that render it soluble in some common aprotic solvents. The chromophore consists of multiple substituted *p*-phenylene vinylene repeat units acting as a single optical unit, i.e., a discrete segment of the polymer backbone. [33,34] Electronic excitations (“excitons”) are localized over these short backbone segments (typically 4–10 monomer units). [4] Shear-induced changes to the nature and environment of the polymer backbone are therefore likely to be reflected in altered fluorescence emission properties. For example, changes in the distribution of conjugation lengths would be observed as changes in maximum absorption and emission wavelengths, and shear-induced orientation should be revealed as a deviation from the quiescent (isotropic) case in polarized emission studies. The intense luminescence observed from MEH-PPV solutions, together with the direct relationship between backbone conformation and emission characteristics anticipated for any conjugated polymer, make MEH-PPV an interesting and appropriate initial candidate for fluorescence studies of polymers in shear flow.

Table I. Matrix Illustrating the Range of MEH-PPV Solutions Studied in This Work

Polymer Solvent	980 k MEH-PPV				133 k MEH-PPV			
	Toluene		Xylene		Xylene		Toluene	
Observation position	A	B	A	B	A	B	A	B
Concentration/ $\mu\text{g ml}^{-1}$	60 ^a	60 ^a	140 ^a		100 ^a	100 ^a		
	30 ^a	30 ^a						
	10 ^a	10 ^a	10 ^a	10 ^a	10 ^a	10 ^a	10 ^a	10 ^a
	5	5						
	1.8	1.8						
	1.5 ^a	1.5						
	1 ^a	1 ^a	1 ^a	1 ^a	1 ^a	1 ^a	1 ^a	1 ^a

^aDenotes depolarization & anisotropy determinations in addition to unpolarized intensity measurements.

Table I identifies the selection of concentrations, solvents and MEH-PPV molecular weights studied in the Couette cell at positions A and B. All solutions were in the “dilute” regime, i.e., at concentrations below the critical overlap concentration, c^* , estimated at $10^{-3} \text{ g}\cdot\text{ml}^{-1}$. [35] Gettinger *et al.* and Cotts reported light scattering studies that indicated MEH-PPV adopts a random coil form in xylene; [35,36] more recent work has also provided evidence of a wide spectrum of conformational states in solutions and films, driven by folding at sp^3 defect sites. [37,38] Polymer chains are regarded as essentially non-interacting in dilute solutions. However, poly[*p*-phenylene vinylene] systems are prone to aggregation owing to π - π^* interactions between adjacent conjugated chains. These intermolecular associations may be observed as additional lower energy (red-shifted) weak bands in the emission spectra. [39] Since the focus of this work was the behavior of isolated MEH-PPV chains in shear we confirmed the absence of these aggregated species in our dilute solutions with steady state absorption and emission spectroscopy.

Table II summarizes steady state spectroscopic properties determined for each of the MEH-PPV solutions. Absorption and emission maxima were invariant for a given polymer molecular weight and solvent. This indicates that the solutions were sufficiently dilute for ag-

gregation effects to be neglected. Additional red-shifted emission bands appeared at higher concentrations, indicating the presence of aggregated species, in accord with previous reports. [39,40]

Figure 3 shows the variation of fluorescence emission intensity as a function of applied shear rate for $1 \mu\text{g}\cdot\text{ml}^{-1}$ 133 k MEH-PPV in toluene. This variation (less than $\pm 2\%$) was typical of all dilute solutions examined in this study. Interestingly, the absolute value of zero shear emission intensity (data not shown) proves to be more imprecise than values recorded in shear. This is because slight off-center positioning of the inner cylinder at rest can result in a changed sample path length that is otherwise averaged by rotation during shear measurements. For example, a $15 \mu\text{m}$ deviation from the central axis corresponds to a 9% difference in the path length of $175 \mu\text{m}$, and therefore a 9% difference in the emission intensity observed from an optically dilute solution. Shear rates were applied in a random order, and no differences were observed between a start/stop regime incorporating quiescent “rest” periods and a continuous cycle of varying shear rates. Extended duration measurements highlighted the effects of spectrometer drift, mainly due to variations in the PMT anode output current during continuous operation. This drift increases the importance of applying shear rates in a random sequence, and limits the experimental timeframe, within which intensity measurements can be reliably compared, to approximately one hour.

We therefore conclude that, within the precision of the measurement, no change in fluorescence intensity attributable to applied shear rate occurs for dilute solutions of MEH-PPV in xylene or toluene.

Figure 4 illustrates fluorescence emission spectra recorded in shear for $30 \mu\text{g}\cdot\text{ml}^{-1}$ 980 k MEH-PPV in toluene at a series of different shear rates. The excitation wavelength was 499 nm for all spectra. The overlaid spectra (inset) emphasize that there is no change in the spectral form of the emission in this shear rate range. This invariance shows that there is no shear-induced deformation of the polymer backbone under these conditions. The invariance of the emission maximum also incidentally

Table II. Summary of Steady State Spectroscopic Properties Determined for All Dilute MEH-PPV Solutions

Polymer Solvent	980 k MEH-PPV		133 k MEH-PPV	
	Toluene	Xylene	Toluene	Xylene
Absorption maximum, $\lambda_{\text{abs, max}}/\text{nm}$	499 \pm 1	499 \pm 1	498 \pm 1	499 \pm 1
Absorption coefficient*, $\epsilon/\text{dm}^3 \text{ mol}^{-1} \text{ cm}^{-1}$	1.4×10^4	—	1.4×10^4	—
Emission maximum, $\lambda_{\text{em, max}}/\text{nm}$	556 \pm 1	555 \pm 1	555 \pm 1	555 \pm 1
Steady state anisotropy, r	0.19	0.18	0.20	0.20

*Absorption coefficient is expressed in terms of monomer unit concentration.

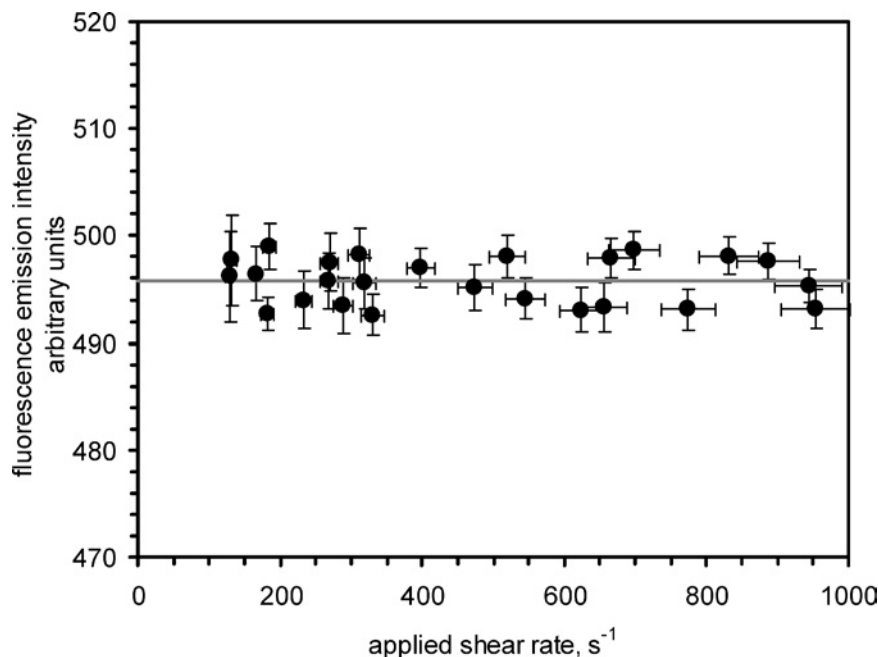


Fig. 3. Variation in fluorescence emission intensity as a function of shear rate. $1 \mu\text{g ml}^{-1}$ 133 k MEH-PPV in toluene, observed at Position A. $\lambda_{\text{ex}} = 499 \text{ nm}$, $\lambda_{\text{em}} = 557 \text{ nm}$. The gray line indicates the mean intensity value. The plot is typical of all dilute MEH-PPV solutions described in this study.

confirms the absence of sample heating: MEH-PPV solutions are strongly thermochromic, and exhibit both a blue shift and a reduced quantum yield at elevated temperatures. Thermal energy introduced to the system as a consequence of the rotational motion of the inner cylinder is effectively dissipated through the quartz block and holder.

Polarized illumination can be employed to further explore the orientation and anisotropy of fluorescent materials as outlined in the introduction. The measurement relies on the preferential excitation of polymer segments whose absorption transition moment is oriented along the electric field vector of the incident beam. [23] This photoselection generates an excited-state population of polymer segments oriented with respect to the polarized light. Shear-induced changes in the orientation distribution of polymer segments should be revealed as shear-dependent changes in the polarized emission intensities. Depolarization may occur via rotational diffusion of segments in the polymer chain, or other energy transfer mechanisms.

Emission anisotropy, r , as defined in Equation (1), is used as a measure of depolarization. A correction factor, G , compensates for unequal detection sensitivities with respect to vertically and horizontally polarized light. The expression for G presented in Equation (1) applies to a 90° format in which excitation and emission channels are mutually perpendicular; a criterion satisfied in our Couette

design. Measurements of fluorescence emission intensity from each polarization combination (VV, VH, HH, HV) were made sequentially while the sample was exposed to a given shear rate, $\dot{\gamma}$. I_{HH} and I_{HV} were used to establish an instantaneous value for $G(\dot{\gamma})$, whereupon I_{VH} & I_{VV} yielded $r(\dot{\gamma})$. This approach compensated for any long-term drift in spectrometer intensity values.

Figure 5 shows steady state emission anisotropy values determined in shear for $10 \mu\text{g}\cdot\text{ml}^{-1}$ 980 k MEH-PPV in xylene, observed across the flow direction in Position A. There is no obvious change in anisotropy across the shear rate range; a uniform finding for all solutions examined in this study. Individual emission intensity trends for each of the V, H polarization combinations were generally consistent with the unpolarized case described above. This invariance further supports the conclusion that no shear-induced orientation of the polymer coils could be detected. It also indirectly confirms our assertion that thermal effects are negligible: sample heating would be observed as an anisotropy change due to a reduction in the rotational correlation time according to the Perrin equation. [23]

We note that the absolute value of r determined in the shear cell is significantly different to that determined in equivalent quiescent solutions in a conventional cuvette (Table II). G factors were similarly distinct. On closer inspection, this was traced to a combination of lensing effects introduced by the cylindrical cell geometry, and

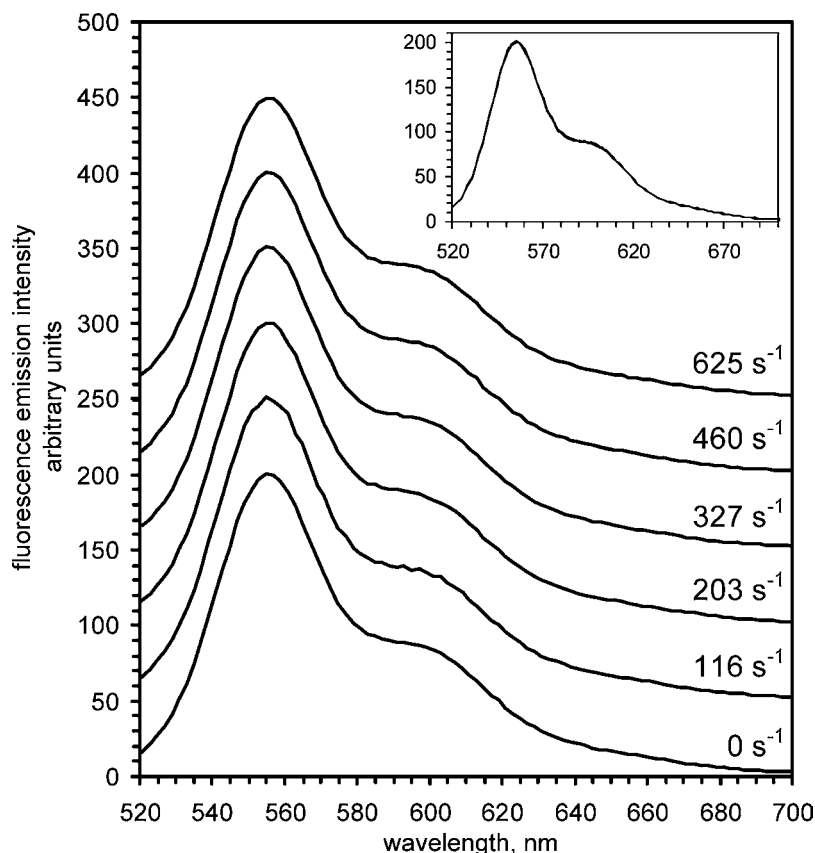


Fig. 4. Uncorrected fluorescence emission spectra recorded at a series of shear rates. $30 \mu\text{g ml}^{-1}$ 980 k MEH-PPV in toluene, observed at Position A, $\lambda_{\text{ex}} = 499 \text{ nm}$. The main graph shows the spectra sequentially offset by 50 units for clarity; the inset shows all six spectra overlaid.

additional scatter from the surface of the Teflon[®] inner cylinder. Fluorescence depolarization measurements are highly susceptible to light scattering. [23] This inhibits quantitative determination of r in the Couette cell; nevertheless shear-induced changes relative to the 0 s^{-1} case can still be observed. The ratiometric nature of the anisotropy calculation does much to eliminate effects of spectrometer drift during the course of an experiment.

A refinement to the anisotropy analysis considers the effect of symmetry breakdown in the flowing system. The conventional expression for r (Equation (1)) assumes cylindrical symmetry of the emission field about the vertical axis. A more complex treatment is required when this symmetry is removed, [41] e.g., by alignment of polymer coils in shear planes. The appropriate expression, and the method for determining it, will be outlined in a subsequent publication. It is not required in this instance as there is no evidence of introduced order or a breakdown of the isotropic case in these solutions.

The singular interpretation of these rheofluorescence measurements is that these dilute MEH-PPV solutions are

insensitive to shear rates in the range $100\text{--}1000 \text{ s}^{-1}$. This is a rather unexpected outcome: a polymer chain in a random coil conformation is anticipated to deform in a steady shear field and align with the flow direction, although large discrepancies do remain between theoretical predictions and experimental observations. [42,43]

The results reported here for commercial MEH-PPV can be interpreted in terms of a polymer configuration that is dominated by chemical and structural defects. Holzer *et al.* recently showed that MEH-PPV synthesized by a commonly-used dehydrohalogenation process, known as the Gilch route, contained up to 30% non-conjugated phenylene-ethylene-phenylene defect units, whilst retaining sufficient polyconjugation to exhibit MEH-PPV-specific absorption and fluorescence characteristics. [44] Gilch-type MEH-PPV was also employed in this study, and ^1H NMR spectra recorded for both polymer samples show additional peaks not described in comparable spectra published for defect-free material. [44,45] It is reasonable to infer that the occurrence of non-conjugated phenylene-ethylene subunits with significant frequency along the

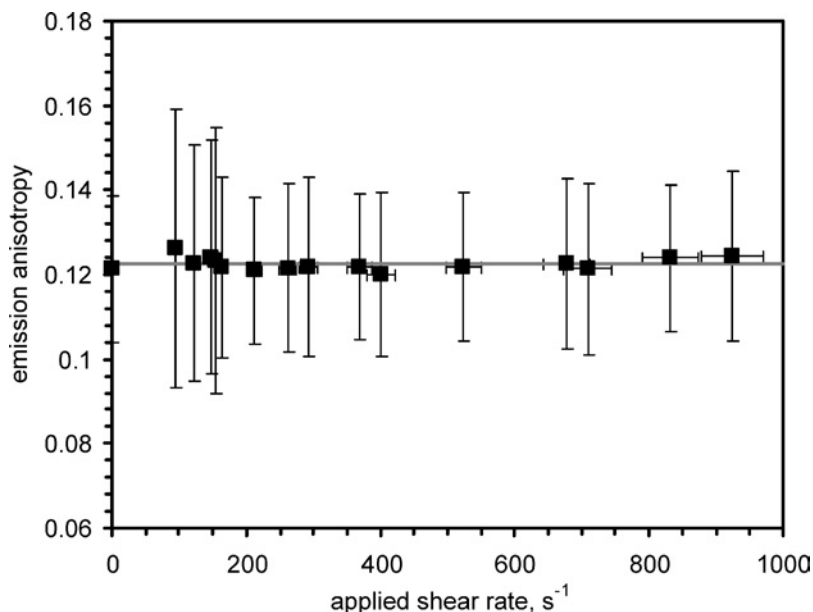


Fig. 5. Steady state emission anisotropy determined in shear for a typical MEH-PPV solution. $10 \mu\text{g ml}^{-1}$ 980 k MEH-PPV in xylene, observed at position A, $\lambda_{\text{ex}} = 499 \text{ nm}$, $\lambda_{\text{em}} = 556 \text{ nm}$. The gray line indicates the mean anisotropy value. See Fig. 2 caption for details of error analysis.

chain dominates the spatial conformation adopted by the polymer. [37] Tetrahedral carbon-carbon links impose “kinks” in the structure and direct folding into semi-stiff, organized configurations less susceptible to shear-induced deformation than the idealized random coil conformation.

Effect of Shear Flow on MEH-PPV Dispersed in Polystyrene Solutions

The absence of an observable shear-induced response in the dilute MEH-PPV solutions described above led us to consider other matrices that might demonstrate a rheofluorescence effect. To this end we prepared a homogeneous dispersion of 133 k MEH-PPV in a concentrated polystyrene solution. Polystyrene is used as a host for conjugated polymers in thin films, is optically inert at the wavelengths of interest and solvates PPV derivatives well. [46,47] Quiescent absorption and emission spectra of the solution were broadly similar to analogous polystyrene-free MEH-PPV solutions; with identical emission maxima, and differences in the ratio of the two vibronic bands. [46]

Figures 6(a) and (b) show shear-dependent changes in maximum emission intensity observed in both cell positions. In contrast to the previous dilute MEH-PPV solutions (Fig. 3), a marked decrease in fluorescence emission observed in Position A is accompanied by a concomitant

increase in emission in Position B. These effects are rapid and reversible over short periods of shear exposure. The changes are related to changes in effective MEH-PPV absorption and emission cross-sections with respect to the optical axes and suggest orientation of the polymer chains in the flow field.

Concentrated polystyrene solutions exhibit strong non-Newtonian behavior, including shear thinning in steady shear flow. This is caused by overall orientation of the polystyrene chains along the flow vector. [48] We believe that the polystyrene matrix acts as a director for MEH-PPV, resulting in shear-induced alignment of the conjugated polymer coils. It is generally accepted that rapid intrachain energy transfer processes dominate MEH-PPV photophysics; [4] the effective emission cross-section consequently governs fluorescence observed at each position in the Couette cell. The trends indicated in Figs. 6(a) and (b) are therefore consistent with prolate polymer objects aligning in shear flow, with their major axis along the flow direction. Furthermore, Fig. 7 compares normalized fluorescence emission spectra recorded before and immediately after shear exposure. Changes in the spectral shape reveal subtle shear-induced deformation in the MEH-PPV coils.

Further work is necessary to fully elucidate this rheological response, but these preliminary data demonstrate the validity of the rheofluorescence method presented in

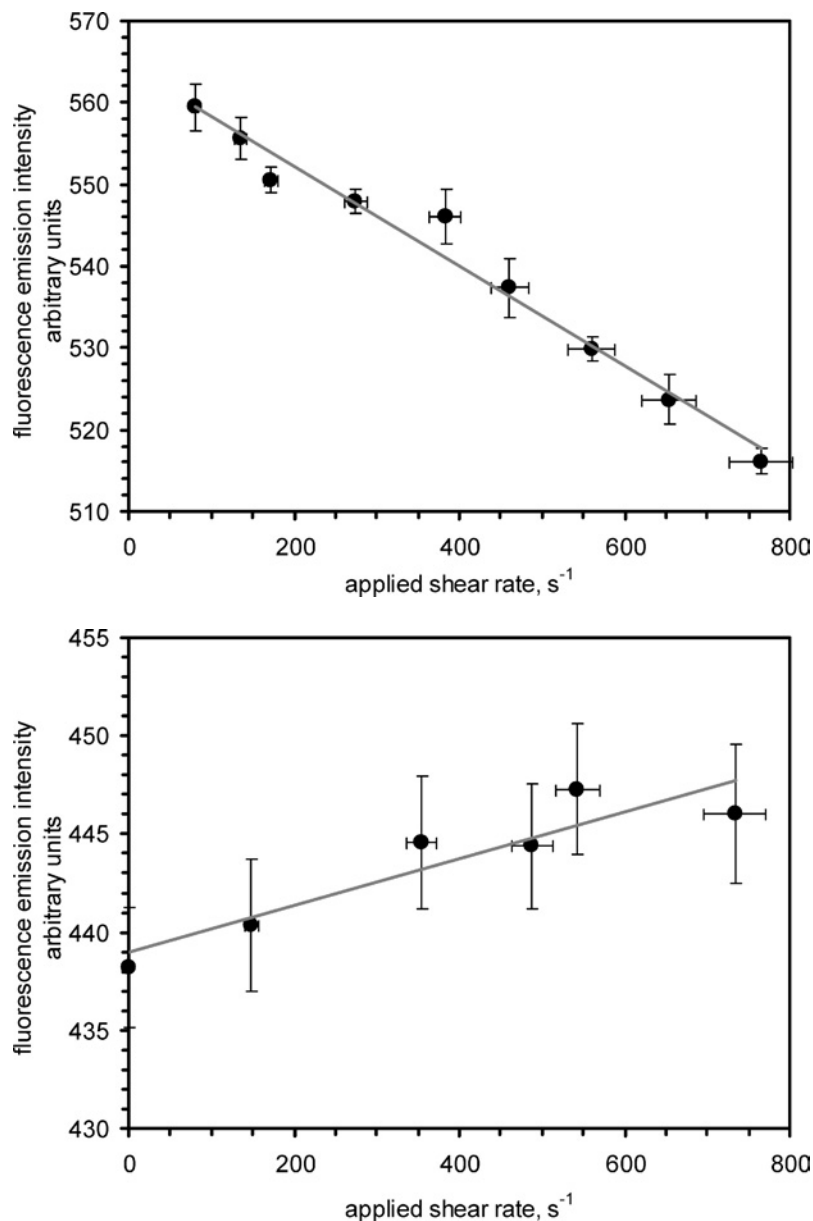


Fig. 6. Shear-induced orientation of MEH-PPV in a concentrated polystyrene solution. 133 k MEH-PPV (1×10^{-3} wt.%) dispersed in 16.2 wt.% polystyrene/toluene, $\lambda_{\text{ex}} = 499$ nm, $\lambda_{\text{em}} = 555$ nm. a) Emission intensity observed at Position A (excitation across flow). b) Emission intensity observed at Position B (excitation along flow). Grey lines indicate best fits by linear regression analysis.

this paper. Shear-induced changes in fluorescence emission are readily observed in this technique.

CONCLUSIONS

A novel optically accessible Couette cell has been used to demonstrate the feasibility and utility of fluorescence measurements of conjugated polymer solutions in

shear flow. The rheofluorescence instrument was characterized with a small molecule, Rhodamine 6G, in solutions of varying viscosity. This dye was anticipated to be unaffected by steady shear flow, and no shear-induced effects were observed in the fluorescence data.

MEH-PPV was adopted as a model light emitting polymer, and studied in dilute solutions spanning two decades of concentration. No shear-induced changes in

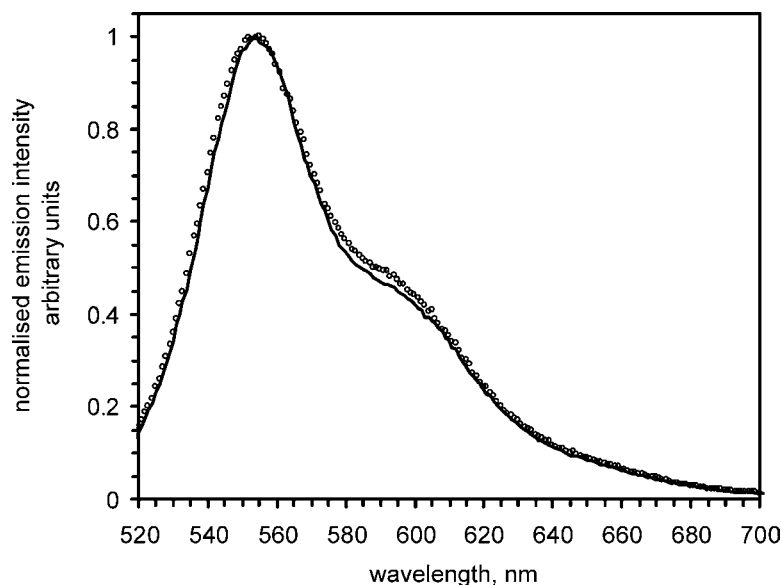


Fig. 7. Comparison of normalized, uncorrected fluorescence emission spectra before and after shear exposure. Solid line: preshear spectrum, hollow circles: postshear spectrum. Sample composition and excitation wavelength were as described in Fig. 6.

fluorescence emission were observed in dilute solutions for rates in the range $100\text{--}1000\text{ s}^{-1}$. We argue that this invariance arises from a polymer conformation driven by chemical and structural defects along the polymer backbone. Initial data obtained by this group for other, defect-free, PPV derivatives supports this view; rheochromism is indeed observed for defect-free material, [49,50] and further work is underway to fully characterize the rheofluorescence response. MEH-PPV dispersed in a concentrated polystyrene solution showed shear-induced orientation and evidence of subtle deformation in shear flow. In this case, the non-Newtonian behavior of the polystyrene matrix surrounding the chains directs the rheological response of the conjugated polymer.

ACKNOWLEDGMENTS

The authors would like to thank Kevin Smeaton for assistance in construction of the shear cell system and Herbert Groiss for manufacturing the quartz cell, Audrey Walewijk for thermochromism studies of MEH-PPV solutions, and Dr Gowri Ramachandran for NMR measurements. Financial support from the Australian Research Council is also gratefully acknowledged.

REFERENCES

1. J. H. Burroughes, D. D. C. Bradley, A. R. Brown, R. N. Marks, K. Mackay, R. H. Friend, P. L. Burns, and A. B. Holmes (1990). Light-emitting diodes based on conjugated polymers. *Nature* **347**(6293), 539–541.
2. R. H. Friend, R. W. Gymer, A. B. Holmes, J. H. Burroughes, R. N. Marks, C. Taliani, D. D. C. Bradley, D. A. dos Santos, J. L. Brédas, M. Lögdlund, and W. R. Salaneck (1999). Electroluminescence in conjugated polymers. *Nature* **397**(6715), 121–128.
3. S. I. E. Vulto, M. Buechel, P. C. Duineveld, F. Dijkman, M. Hack, M. Kilitziraki, M. M. de Kok, E. A. Meulenkaamp, J.-E. J. M. Rubingh, P. van de Weijer, and S. H. de Winter (2004). Technology and materials for full-color polymer light-emitting displays. *Proc. SPIE* **5214**, 40–49.
4. B. J. Schwartz (2003). Conjugated polymers as molecular materials: How chain conformation and film morphology influence energy transfer and interchain interactions. *Annu. Rev. Phys. Chem.* **54**(1), 141–172.
5. J. Kim (2002). Assemblies of conjugated polymers. Intermolecular and intramolecular effects on the photophysical properties of conjugated polymers. *Pure Appl. Chem.* **74**(11), 2031–2044.
6. B.-J. de Gans, P. C. Duineveld, and U. S. Schubert (2004). Inkjet printing of polymers: State-of-the-art and future developments. *Adv. Mater.* **16**(3), 203–213.
7. R. G. Larson (1999). *The Structure and Rheology of Complex Fluids*. Oxford University Press, New York.
8. M. Doi and S. F. Edwards (1986). *The theory of polymer dynamics*. Oxford University Press, Oxford.
9. P. G. de Gennes (1991). *Scaling Concepts in Polymer Physics*. Cornell University Press, Ithaca.
10. D. E. Dunstan, E. K. Hill, and Y. Wei (2004). Direct measurement of polydiacetylene 4-butoxycarbonylmethylurethane segment orientation and distortion in shear: Semi-dilute solutions. *Macromolecules* **37**(4), 1663–1665.
11. S. J. Gason, D. E. Dunstan, T. A. Smith, D. Y. C. Chan, L. R. White, and D. V. Boger (1997). Rheooptical studies of polydiacetylene solutions. *J. Phys. Chem. B* **101**(39), 7732–7735.
12. S. J. Gason, J. Cooper-White, D. E. Dunstan, and D. V. Boger (2001). A spectroscopic study of polyelectrolyte solutions under shear. *Polymer* **42**, 6981–6989.

13. M. A. Winnik (1986). In *N.A.T.O. A.S.I. Series, Series C, Mathematical and Physical Sciences*, vol. 182, D. Reidel Publishing Company, Dordrecht.
14. L. Monnerie (1985). In D. Phillips (Ed.), *Polymer Photophysics*, Chapman and Hall, London, UK, pp. 279–339.
15. H. Zettl, W. Hafner, A. Boker, H. Schmalz, M. Lanzendorfer, A. H. E. Muller, and G. Krausch (2004). Fluorescence Correlation Spectroscopy of single dye-labeled polymers in organic solvents. *Macromolecules* **37**(5), 1917–1920.
16. G. G. Fuller (1995). *Optical Rheometry of Complex Fluids*. Oxford University Press, New York.
17. A. J. Bur, R. E. Lowry, S. C. Roth, C. L. Thomas, and F. W. Wang (1991). Observations of shear-induced molecular orientation in a polymer melt using fluorescence anisotropy measurements. *Macromolecules* **24**(12), 3715–3717.
18. S. Mani, M. F. Malone, H. H. Winter, J. L. Halary, and L. Monnerie (1991). Effects of shear on miscible polymer blends: In situ fluorescence studies. *Macromolecules* **24**(19), 5451–5458.
19. D. E. Smith, H. P. Babcock, and S. Chu (1999). Single-polymer dynamics in steady shear flow. *Science* **283**(5408), 1724–1727.
20. P. le Duc, C. Haber, G. Bao, and D. Wirtz (1999). Dynamics of individual flexible polymers in a shear flow. *Nature* **399**(6736), 564–566.
21. Y. Wang, A. Warshawsky, C. Wang, N. Kahana, C. Chevillard, and V. Steinberg (2002). Fluorescent ultrahigh-molecular-weight polyacrylamide probes for dynamic flow systems: synthesis, conformational behaviour and imaging. *Macromol. Chem. Phys.* **203**(12), 1833–1843.
22. C. W. Macosko (1994). *Rheology: Principles, Measurements and Applications*. VCH Publishers Inc, New York.
23. J. R. Lakowicz (1999). *Principles of Fluorescence Spectroscopy*. Kluwer Academic/Plenum, NY.
24. F. Cacialli (1999). Conjugated and electroluminescent polymers. *Curr. Opin. Colloid & Interface Sci.* **4**(2), 159–164.
25. T.-Q. Nguyen, V. Doan, and B. J. Schwartz (1999). Conjugated polymer aggregates in solution: Control of interchain interactions. *J. Chem. Phys.* **110**(8), 4068–4078.
26. K. Walters (1975). *Rheometry*. Chapman & Hall, London.
27. S. J. Gason (2001). A spectroscopic study of macromolecular solutions and particulate suspensions under shear, PhD Thesis, University of Melbourne, Melbourne, Australia.
28. S. J. Muller, R. G. Larson, and E. S. G. Shaqfeh (1989). A purely elastic transition in Taylor-Couette flow. *Rheol. Acta* **28**, 499–503.
29. R. F. Kubin and A. N. Fletcher (1983). Fluorescence quantum yield of some rhodamine dyes. *J. Lumin.* **27**(4), 455–462.
30. G. Porter, P. J. Sadkowski, and C. J. Tredwell (1977). Picosecond rotational diffusion in kinetic and steady state fluorescence spectroscopy. *Chem. Phys. Lett.* **49**(3), 416–420.
31. K. A. Selanger, J. Falnes, and T. Sikkeland (1977). Fluorescence lifetime studies of Rhodamine 6G in methanol. *J. Phys. Chem.* **81**(20), 1960–1963.
32. V. E. Korobov and A. K. Chibisov (1978). Primary processes in the photochemistry of rhodamine dyes. *J. Photochem.* **9**(5), 411–424.
33. W. Holzer, A. Penzkofer, S.-H. Gong, D. D. C. Bradley, X. Long, and A. Bleyer (1997). Effective stimulated emission and excited-state absorption cross-section spectra of poly(m-phenylenevinylene-co-2,5-dioctoxy-p-phenylenevinylene) and *t-t'*-didecyloxy-II-distyrylbenzene. *Chem. Phys.* **224**, 315–326.
34. J. L. Brédas, J. Cornil, D. Beljonne, D. A. dos Santos, and Z. Shuai (1999). Excited-state electronic structure of conjugated oligomers and polymers: A quantum-chemical approach to optical phenomena. *Acc. Chem. Res.* **32**(3), 267–276.
35. C. L. Gettinger, A. J. Heeger, J. M. Drake, and D. J. Pine (1994). A photoluminescence study of poly(phenylenevinylene) derivatives: The effect of intrinsic persistence length. *J. Chem. Phys.* **101**(2), 1673–1678.
36. P. M. Cotts (1997). Molecular weight distribution and configuration of MEH-PPV in dilute solution. *Polym. Preprints* **38**(1), 355–356.
37. D. Hu, J. Yu, K. Wong, B. Bagchi, P. J. Rossky, and P. F. Barbara (2000). Collapse of stiff conjugated polymers with chemical defects into ordered, cylindrical conformations. *Nature* **405**(6790), 1030–1033.
38. P. Kumar, T.-H. Lee, A. Mehta, B. Sumpter, R. M. Dickson, and M. D. Barnes (2004). Photon antibunching from oriented semiconducting polymer nanostructures. *J. Am. Chem. Soc.* **126**(11), 3376–3377.
39. T.-Q. Nguyen, I. B. Martini, J. Liu, and B. J. Schwartz (2000). Controlling interchain interactions in conjugated polymers: The effects of chain morphology on exciton-exciton annihilation and aggregation in MEH-PPV films. *J. Phys. Chem. B* **104**(2), 237–255.
40. M. Zheng, F. Bai, and D. Zhu (1998). Photophysical process of MEH-PPV solution. *J. Photochem. Photobiol. A* **116**, 143–145.
41. J. Kusba and J. R. Lakowicz (1999). Definition and properties of the emission anisotropy in the absence of cylindrical symmetry of the emission field: Application to the light quenching experiments. *J. Chem. Phys.* **111**(1), 89–99.
42. R. B. Bird, C. F. Curtis, R. C. Armstrong, and O. Hassager (1987). *Dynamics of polymeric liquids: Kinetic Theory*. Wiley Interscience, New York.
43. A. Link and J. Springer (1993). Light scattering from dilute polymer solutions in shear flow. *Macromolecules* **26**(3), 464–471.
44. W. Holzer, A. Penzkofer, H. Tillmann, and H.-H. Hörhold (2004). Spectroscopic and travelling-wave lasing characterisation of Gilch-type and Horner-type MEH-PPV. *Synthetic Met.* **140**(2–3), 155–170.
45. C. J. Collison, L. J. Rothberg, V. Treemanekarn, and Y. Li (2001). Conformational effects on the photophysics of conjugated polymers: A two species model for MEH-PPV spectroscopy and dynamics. *Macromolecules* **34**(7), 2346–2352.
46. S. S. Sartori, S. De Feyter, J. Hofkens, M. van der Auweraer, and F. C. De Schryver (2003). Host matrix dependence on the photophysical properties of individual conjugated polymer chains. *Macromolecules* **36**(2), 500–507.
47. W. Holzer, M. Pichlmaier, A. Penzkofer, D. D. C. Bradley, and W. J. Blau (1999). Fluorescence spectroscopic behaviour of neat and blended conjugated polymer thin films. *Chem. Phys.* **246**, 445–462.
48. D. Yavich, D. W. Mead, J. P. Oberhauser, and L. G. Leal (1998). Experimental studies of an entangled polystyrene solution in steady state mixed type flows. *J. Rheol.* **42**(3), 671–695.
49. E. K. Hill, K. L. Chan, A. B. Holmes, and D. E. Dunstan (2004). “Fluorescence spectroscopy of poly(p-phenylenevinylene) derivatives in flow,” presented at International Conference on Synthetic Metals, ICSM’04, Wollongong, NSW.
50. E. K. Hill, K. L. Chan, A. B. Holmes, and D. E. Dunstan (2005). Rheofluorescence studies of poly(p-phenylenevinylene) derivatives in simple shear flow. *Synthetic Met.* (in press).